SANDIA REPORT

SAND2004-4845
Unlimited Release
Printed October 2004

A Capillary Valve for Microfluidic Systems

Michael P. Kanouff, Brian M. Rush, and Eric B. Cummings

Prepared by
Sandia National Laboratories
Albuquerque, New Mexico 87185 and Livermore, California 94550

Sandia is a multiprogram laboratory operated by Sandia Corporation,
a Lockheed Martin Company, for the United States Department of Energy's
National Nuclear Security Administration under Contract DE-AC04-94-AL85000.

Sandia National Laboratories

Issued by Sandia National Laboratories, operated for the United States Department of Energy by Sandia Corporation.

Available to DOE and DOE contractors from
U.S. Department of Energy
Office of Scientific and Technical Information
P.O. Box 62
Oak Ridge, TN 37831

Telephone: (865) 576-8401
Facsimile: (865) 576-5728
E-Mail: reports@adonis.osti.gov
Online ordering: http://www.doe.gov/bridge

Available to the public from
U.S. Department of Commerce
National Technical Information Service
5285 Port Royal Rd
Springfield, VA 22161

Telephone: (800) 553-6847
Facsimile: (703) 605-6900
E-Mail: orders@ntis.fedworld.gov
Online order: http://www.ntis.gov/help/ordermethods.asp?loc=7-4-0#online

SAND2004-4845
Unlimited Release
Printed October 2004

A Capillary Valve for Microfluidic Systems

Michael P. Kanouff, Brian M. Rush
Fluid and Thermal Science Department

and

Eric B. Cummings
Microfluidics Department

Sandia National Laboratories
P.O. Box 969
Livermore, California 94551-0969

ABSTRACT

Microfluidic systems are becoming increasingly complicated as the number of applications grows. The use of microfluidic systems for chemical and biological agent detection, for example, requires that a given sample be subjected to many process steps, which requires microvalves to control the position and transport of the sample. Each microfluidic application has its own specific valve requirements and this has precipitated the wide variety of valve designs reported in the literature. Each of these valve designs has its strengths and weaknesses. The strength of the valve design proposed here is its simplicity, which makes it easy to fabricate, easy to actuate, and easy to integrate with a microfluidic system. It can be applied to either gas phase or liquid phase systems. This novel design uses a secondary fluid to stop the flow of the primary fluid in the system. The secondary fluid must be chosen based on the type of flow that it must stop. A dielectric fluid must be used for a liquid phase flow driven by electroosmosis, and a liquid with a large surface tension should be used to stop a gas phase flow driven by a weak pressure differential.

Experiments were carried out investigating certain critical functions of the design. These experiments verified that the secondary fluid can be reversibly moved between its 'valve opened' and 'valve closed' positions, where the secondary fluid remained as one contiguous piece during this transport process. The experiments also verified that when Fluorinert is used as the secondary fluid, the valve can break an electric circuit. It was found necessary to apply a hydrophobic coating to the microchannels to stop the primary fluid, an aqueous electrolyte, from wicking past the Fluorinert and short-circuiting the valve. A simple model was used to develop valve designs that could be closed using an electrokinetic pump, and re-opened by simply turning the pump off and allowing capillary forces to push the secondary fluid back into its stowed position.

Intentionally Left Blank

TABLE OF CONTENTS

LIST OF FIGURES

Intentionally Left Blank

A Capillary Valve for Microfluidic Systems

1. Introduction

As microfluidics takes on increasingly challenging applications microfluidic systems are becoming increasingly complex. A prime example is the application of microfluidics to chemical and biological agent detection. This is clearly of critical importance, but it is a daunting task because deadly agents can be easily masked by the relatively large concentration of benign ambient particles normally present in the atmosphere. Consequently, a complex set of processes must be carried out beginning with a process for sorting the particles based on chemical and biological signatures. This decreases the size of the sample that must be tested. Other steps in the detection of chemical and biological agents include lysing the presorted particles and subjecting their contents to multiple assays. These processes can be done in either the gas or liquid phases, but either way valves will invariably be required to control the location of a sample on a chip to carry out these processes.

There is a wide range of applications calling for microvalves and each one has its own set of requirements. No one valve design is likely to meet all of them. This is reflected in the wide variety of microvalve designs that have been reported (see Chapter 2). But there is one set of requirements that all designs should meet. They should be chemically inert to samples, inexpensive to fabricate, easily actuated (preferably by an electronic signal), and small and topologically convenient so that they can become an integral part of the microfluidic system. Valves that meet these requirements will make it possible to take full advantage of microfluidic systems, one of which is to mass produce sophisticated and complex processing systems economically. The operational mechanism of the microvalve we are proposing is exceptionally simple and scales favorably to microscales. Hence these valves should be easy and inexpensive to build and employ at the micro scale. This novel design uses one fluid to stop another. Other than the secondary fluid, there are no moving parts. This valve should be easy to integrate with a microfluid system because it is just another microfluidic circuit. It can be applied to either gas or liquid phase systems to stop either electroosmotic flow or flow driven by weak pressure differentials.

In this one-year feasibility study we used models to identify viable designs and carried out experiments to explore physical limitations of the valve concept. The experiments were directed primarily towards the application of the valve to a liquid phase system. The experiments verified that Fluorinert in a microchannel can break an electrical circuit, which will stop an electroosmotic flow. They also verified that a secondary fluid (immiscible with the primary fluid) can be moved between a stowed position and a position where it can stop the flow of the primary fluid reversibly while remaining in one contiguous piece. A simple model was used to quantify the forces that act on the fluid used to block the primary flow. The model was used to calculate the pressure required to actuate the valve and to design microchannels that result in capillary forces that help control the movement and position of the secondary fluid.

Intentionally Left Blank

2. Background

Many types of micro valves have been reported in the literature ranging from intricate assemblies of micro-machined silicon parts, such as the valve designed by Strobelt et al. [1], to simpler designs that can be directly integrated into the microchip. Only the latter are of interest here. Valves of this type require microscale designs that are usually restricted to primitive techniques. For example, Man et al. [2] used a channel geometry with a neck or constriction in it to stop an advancing liquid meniscus by capillary forces. Lee et al. [3], and Andersson et al. [4], created hydrophobic surfaces in channels and used them to stop an advancing liquid meniscus due to a change in contact angle. Yu et al. [5] developed valves based on a soft and elastic hydrogel that actuated autonomously when exposed to certain types of liquids. Hasselbrink et al. [6] developed a valve based on a moving micropiston created in situ by laser polymerization. The piston is pushed up against a valve seat to stop a flow driven by high pressure. Each of these designs has its weakness, whether it is a limitation on its functionality, a poor performance, an expensive fabrication process, or a low yield fabrication process.

The valve design investigated here also has its strengths and weaknesses. A strength is its size scaling and simplicity, which makes it easy to fabricate, function and integrate within a microsystems. A weakness is the limited pressure differential that it can support, although this pressure increases as the valve size decreases. In fact, the ultimate application of this design may be at the nanoscale.

Intentionally Left Blank

3. Description of the Valve

The valve design studied here uses a secondary fluid to control the flow of the primary fluid in a microfluidic channel. The valve is open when the secondary fluid is stowed in a side branching channel allowing the primary fluid to pass through the main channel, as shown in Figure 1a. Figure 1b shows the valve in the closed position where the secondary fluid has been pushed into the main channel to block the flow of the primary fluid. In the closed position the secondary fluid is held in place by a combination of capillary, pressure and perhaps other forces of electrical origin.

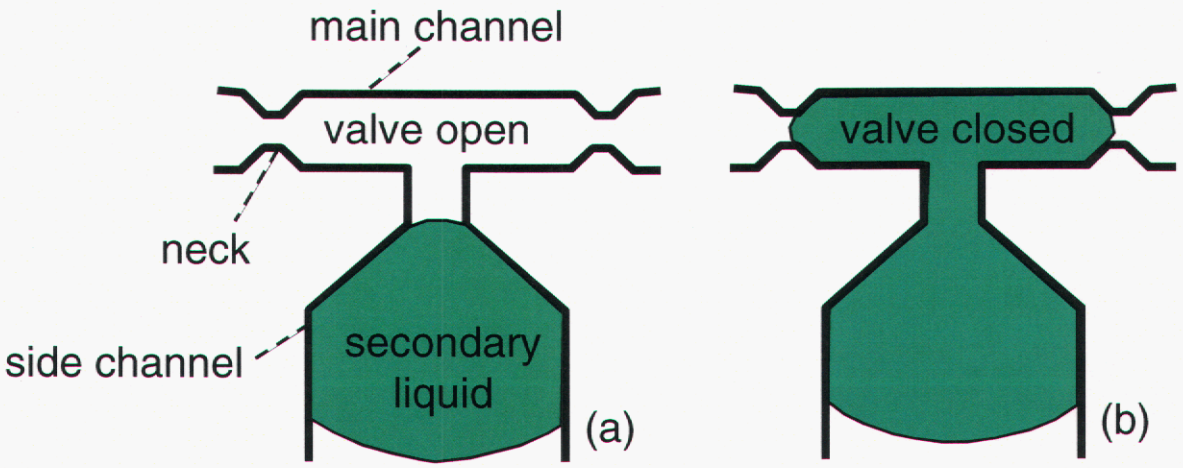

Figure 1. A schematic diagram of the capillary valve.

In the case of liquid phase systems driven by electroosmosis the secondary fluid must be a dielectric, which could be either an insoluble gas or an immiscible liquid. By displacing the primary fluid with the dielectric over some small region in the channel the electric circuit driving the flow is broken and the electroosmotic flow is stopped. Due to the small scale of the systems under consideration here the secondary fluid only extends over a small distance of the channel. Consequently, the voltage gradient across the secondary fluid will be large even for modest voltage potential differences. This requires fluids with large dielectric strengths, which include sulfur hexafluoride (SF_6, gas, 9000 V/mm) and Fluorinert ([7], liquid, 16500 V/mm). In the case of a gas phase system the secondary fluid should be a liquid with a large surface tension, e.g. mercury.

The valve could be activated by a number of different techniques. An electrokinetic (EK) pump connected to the side branching channel could be used to raise the pressure behind the secondary fluid pushing it into the main channel as shown in Figure 2. The secondary fluid would be held in place by a combination of capillary forces and the elevated pressure created by the EK pump. To re-open the valve the EK pump would be turned off allowing the capillary forces to push the secondary fluid out of the main channel and back into the side branching channel. There are also some novel electrical effects on capillary phenomena that may be used to actuate the valve. These include effects on the surface tension (electrocapillary, [8]), effects on the contact angle (electro-wetting) and dielectrophoretic forces that act on a dielectric due to a non-uniform electric field. Kim [9] obtained a liquid velocity of 10 cm/s using an electro-wetting technique.

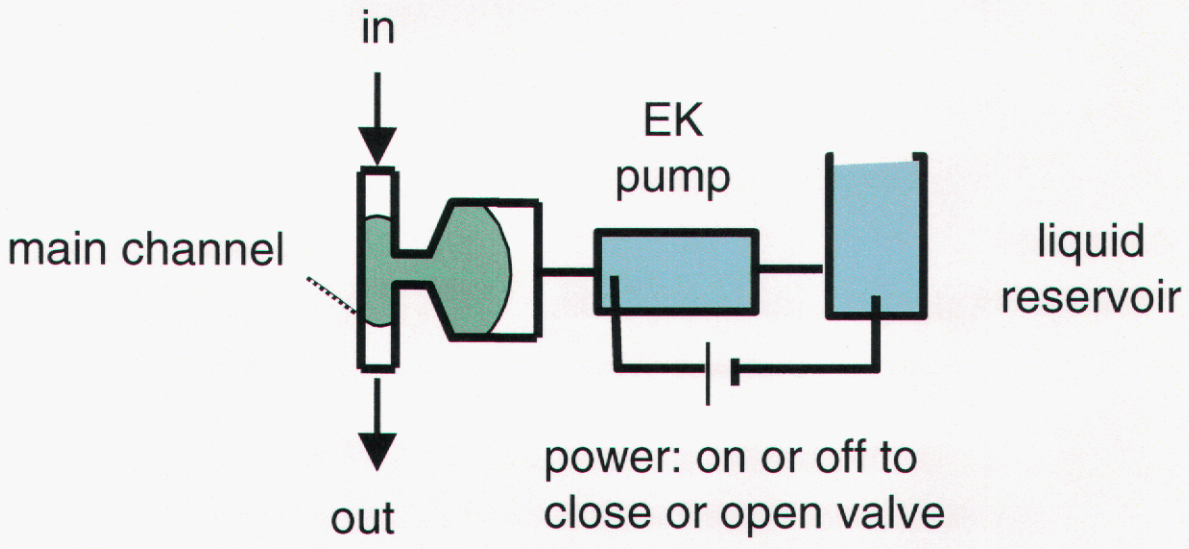

Figure 2. A schematic diagram showing an electrokinetic pump for actuating the valve.

4. Theory

The valve concept studied here involves the static and dynamic behavior of a multi-fluid system in a microchannel. This behavior is governed by the Navier-Stokes equations and associated boundary conditions which account for a large number of complex physical phenomena in their most general form. Much can be learned about the relative importance of these phenomena by simply examining the values of the dimensionless numbers obtained by scaling the governing equations. Four of these dimensionless numbers that are of interest here are shown in Equation 1, the Bond number, Bo, the Capillary number, Ca, and the Weber number, We. The Reynolds number is not independent and is given by, Re = We/Ca. The dimensionless numbers are defined in terms of a length scale, L, the acceleration of gravity, g, the fluid velocity, V, the fluid density, ρ, the surface tension, γ, and the fluid viscosity, μ.

$$Bo = \frac{\rho g L^2}{\gamma}, \; Ca = \frac{\mu V}{\gamma}, \; We = \frac{\rho L V^2}{\gamma} \tag{1}$$

Aqueous solutions are often used in microfluidic systems for chemical and biological agent detection, so the properties of water (ρ = 1 g/cc, γ = 73 g/s^2, and μ = 0.0098 g/cm/s) were used to evaluate the dimensionless numbers. The value chosen for L depends on the specific area of interest. There are two vastly different length scales present in microfluidic systems, one representing the lateral dimension of a microchannel, around 20 μm, and one representing the length of a microchannel, around 10 cm. To identify the important phenomena affecting the shape of aqueous interfaces a length scale representing the channel width should be used, i.e. L = 20 μm. Also, a value for the fluid velocity was used that would result in rapid actuation of the valve. A value of V = 1 cm/s gives an actuation time of 0.01 s for a distance of 100 μm that the secondary fluid would have to traverse.

Using the properties and scales discussed above, the values obtained for the dimensionless numbers are Bo = $5 \cdot 10^{-5}$, Ca = 10^{-4}, and We = $3 \cdot 10^{-5}$ (Re = 0.3). The small values of Bo, Ca and We indicate that gravitational, viscous and inertial forces within the fluid are all negligible compared to the surface tension force. Thus, the shape of an interface will not be significantly affected by these forces and it should have a uniform curvature. This simplifies the theory required to predict the shape of fluid interfaces. Among other simplifications, the curvature will be uniform over any one interface and determined by the channel geometry and the contact angle of the interface with the channel walls. Note that this analysis applies only to forces acting over the small length scale representative of a fluid interface in a microchannel, which will be approximately equal to the channel width. If the channel length is considered it would be necessary to include an aspect ratio which would show that viscous and graviatational forces can be important to the flow rate of fluid through the chip.

Curvature is defined as the inverse of the radius of curvature. The radius of curvature, R, for an interface in a channel with a rectangular cross section in terms of the contact angle, θ, and the channel width, w, and height, h, is given by Equation 2 [10]. This equation for R is related to the more customary method of expressing curvature in terms of two orthogonal radii of curvature, r_1 and r_2, by $2R^{-1} = r_1^{-1} + r_2^{-1}$. The pressure difference that this curvature will induce across the interface is given by the Laplace equation, which takes the form of Equation 3 when using Equation 2 for the curvature. Note that the fluid pressure is always higher on the concave side of the curved interface. As the channel cross-sectional dimensions get smaller, R gets smaller and Δp gets larger.

$$R = \left[\cos\theta\left(\frac{1}{w} + \frac{1}{h}\right)\right]^{-1} \tag{2}$$

$$\Delta p = \frac{2\gamma}{R} \tag{3}$$

Consider a channel with a large value of h and a step change in w as shown in Figure 3a. The channel is filled with one fluid everywhere except for the region spanning the step change, where a second fluid is located as shown. Equations 2 and 3 can be used to show that to maintain the second fluid in this position there must be a pressure difference across it given by, $\Delta p = 2\gamma\cos\theta(w_1^{-1} - w_2^{-1})$. That is, if this pressure differential does not exist then the second fluid would move to the right until its left interface is outside of the region with small width. Similarly, if a neck exists in a channel as shown in Figure 3b, then the pressure differential equal to or greater than that given above would be required to push the second fluid through the neck. If the pressure differential were less than this then the second fluid would stop at the neck and there would be no flow inspite of a non-zero pressure differential.

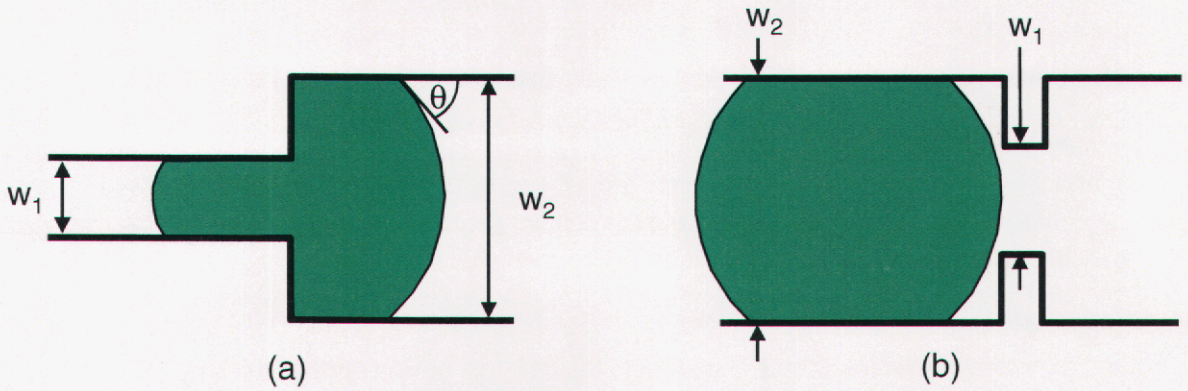

Figure 3. Immiscible fluid plug positioned a) at step change and b) near neck in channel width.

Note that a sharp corner on a solid surface will behave as a hinge for the contact point of an interface. That is, as shown in Figure 4, an interface may have a range of curvatures when in contact with a sharp corner and still satisfy the contact angle requirement. This is because a

corner will actually have a non-zero radius to it, as shown in the figure. The contact point of an interface need only traverse a small distance along such a surface in order for the slope or orientation of the interface to change by a large amount.

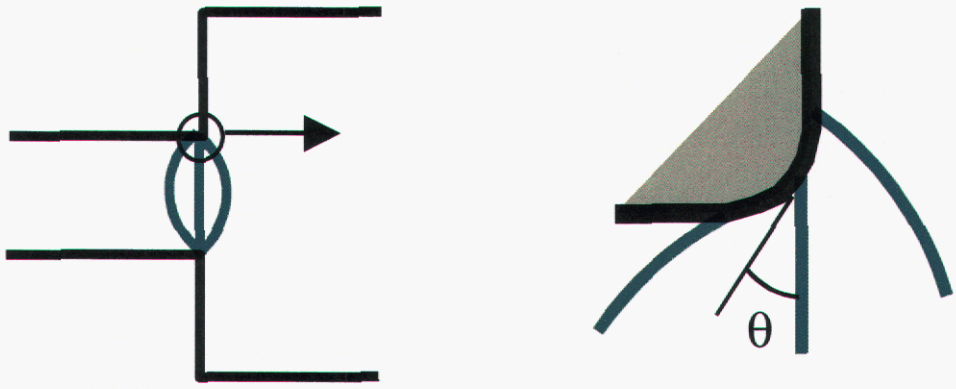

Figure 4. A sharp corner behaving as a hinge for an interface.

The sequence of pressure differences, p_3-p_1, required to hold a secondary fluid in various positions in two different channel designs were calculated using Equations 2 and 3 along with some of the principles discussed above. Figure 5 graphically shows the relationship across the various fluid interfaces.

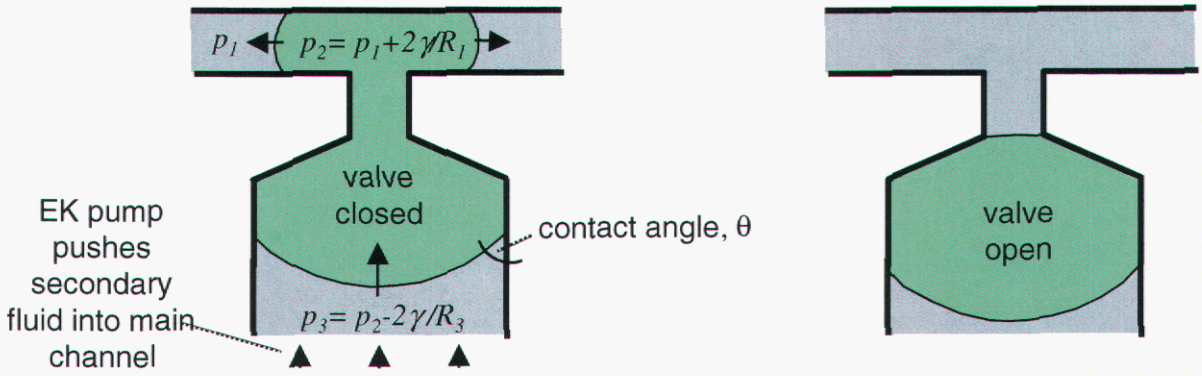

Figure 5. A schematic diagram showing the relationships between pressures in the main channel, p_1, the secondary fluid, p_2, and the side channel, p_3.

Figure 6 shows results for a large aspect ratio geometry where the channel height is much larger than its width. Figure 7 shows results for a low aspect ratio geometry where the height is smaller than the width. These results show that the secondary fluid could be pushed into and held in the main channel by simply raising the pressure in the side channel up to a pre-set value (e.g. 2000 Pa for the high aspect ratio design, and 8000 Pa for the low aspect ratio design), and that capillary forces would push the secondary fluid back out of the main channel by simply lowering the pressure difference to zero. That is, due to the smaller widths and/or heights in the main channel compared to the side channel, the fluid with a contact angle less than 90^{o} will move to the side channel when not forced to do otherwise.

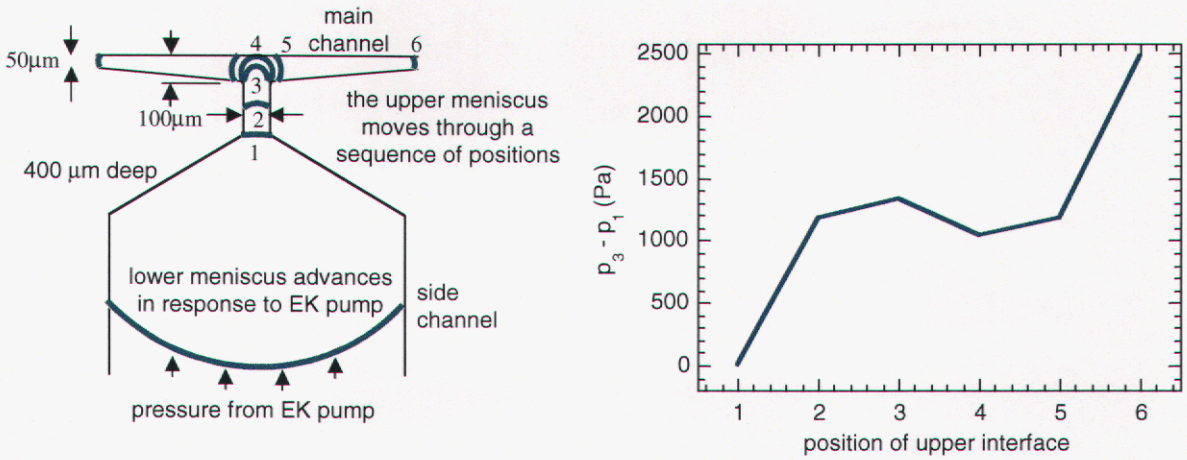

Figure 6. The pressure difference between the side and main channels required to hold the secondary fluid in various positions for high aspect ratio microchannels.

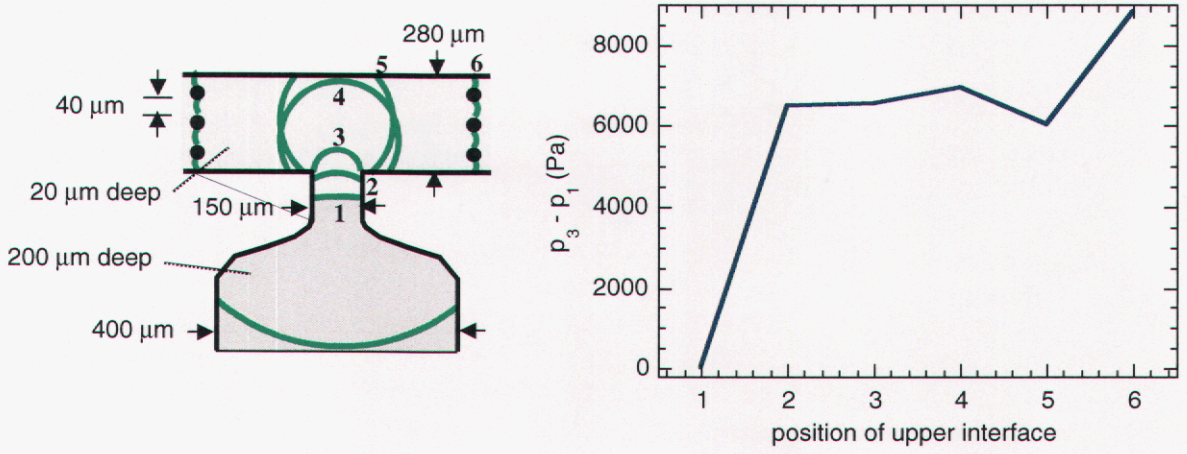

Figure 7. The pressure difference between the side and main channels required to hold the secondary fluid in various positions for low aspect ratio microchannels.

A secondary fluid can also hold off a small pressure differential in the main channel if it has the right shape, as was discussed for Figure 3a. For example, consider the high aspect ratio design shown in Figure 6. Note that the main channel in the vicinity of its junction with the side channel is tapered. This results in an interface curvature that is dependent on its distance from the junction. Consider an upstream pressure, p_{up}, in the main channel that is greater than the downstream pressure, p_{down}. The upstream interface would be located in a position closer to the junction where the channel width is larger, and the downstream interface would be located further from the junction where the channel width is smaller, as shown in Figure 8. The maximum pressure differential that could be supported by this design is 832 Pa for water as the secondary fluid, and it is 5695 Pa (23 inch of H_2O) for mercury as the secondary fluid. These pressure differentials are not large, but they do not have to be for many of the gas phase and liquid phase systems of interest.

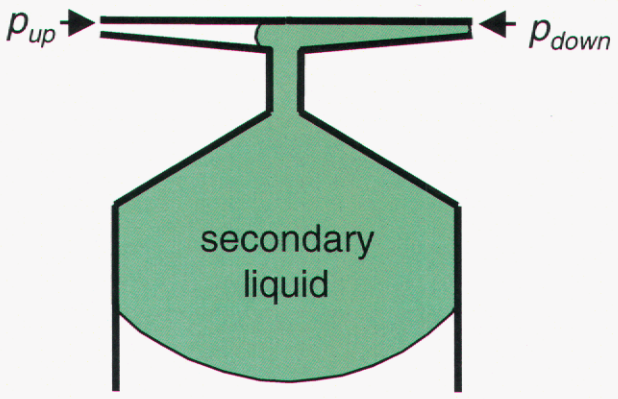

secondary liquid	p_{up}-p_{down}
water	832 Pa
mercury	5695

Figure 8. A schematic diagram showing the relative positions of the upstream and downstream fluid interfaces that support a pressure differential in the main channel.

Intentionally Left Blank

5. Experiments

Experiments were carried out to investigate the reversibility of moving a secondary fluid from a side channel to a main channel in a microchip. Figure 9 shows a schematic diagram of the system used to control the movement and positioning of the secondary fluid. The chip was first loaded with water containing Fluorescein, a fluorescent liquid that helped distinguish between the water and Fluorinert. A vial of secondary fluid, in this case Fluorinert, was connected to the side channel with a capillary. The vial was elevated to force Fluorinert into the chip by gravitational forces. When the Fluorinert reached a targeted position the vial was lowered to the elevation of the chip to stop the flow. It was withdrawn by lowering the vial relative to the chip. The position of the Fluorinert in the chip was monitored using a microscope.

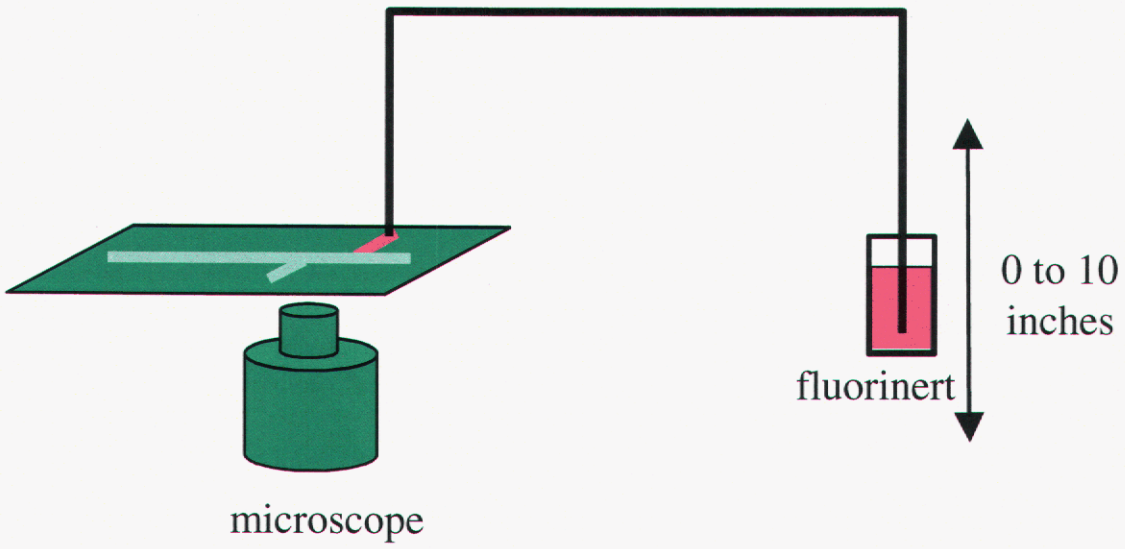

Figure 9. A schematic diagram of the experimental set up for investigating the reversibility of pushing a secondary fluid out of the side channel and into the main channel.

Figure 10 shows a sequence of images captured with a microscope during the movement of Fluorinert out of the side channel and into the main channel. The first two frames of Figure 10 show the fluoresence of the Fluorescein when excited by ultraviolet light, clearly distinguishing the aqueous solution from the Fluorinert. The Fluorinert was pushed into the main channel and withdrawn many times to verify the reversibility of this movement. No detectable trace of Fluorinert was left behind in the main channel.

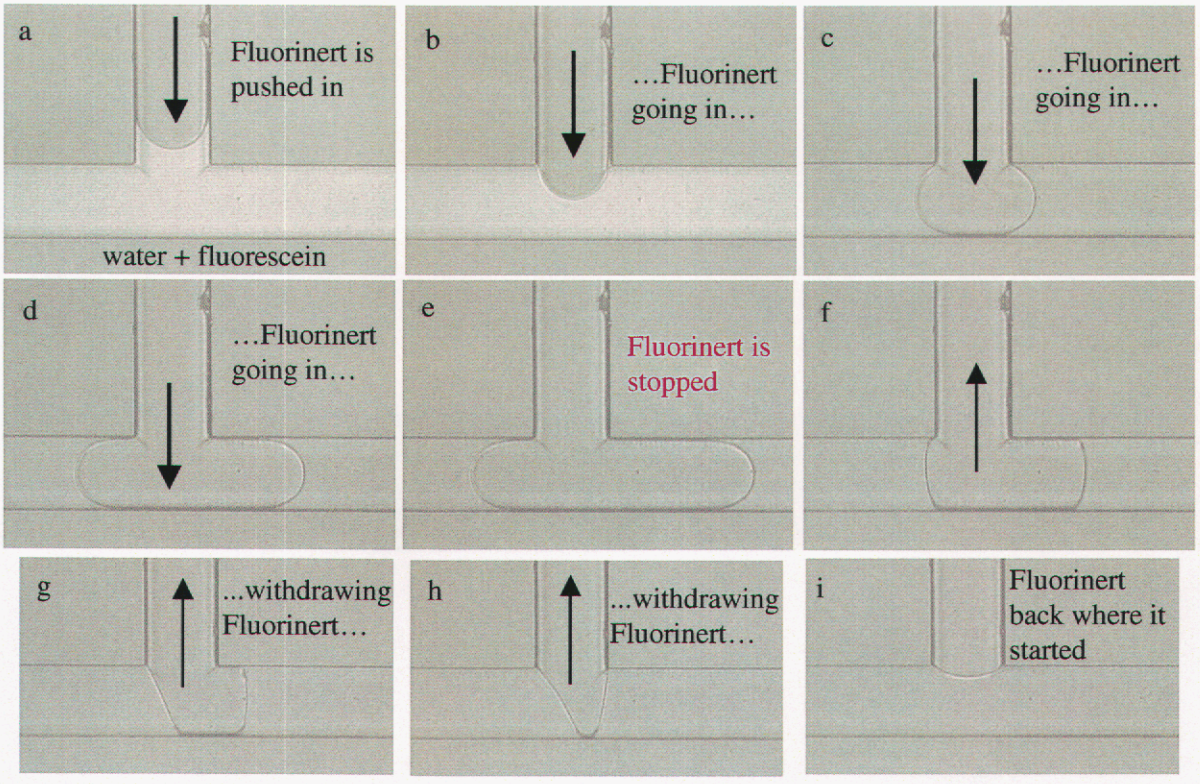

Figure 10. Photomicrographs showing the position of the Fluorinert/water interfaces as the Fluorinert is pushed out of a side channel and into a main channel, followed by withdrawing the Fluorinert back into the side channel.

Note the direction of curvature of the interface between the Fluorinert and water in Figure 10, it is concave towards the Fluorinert indicating that water wets glass better than Fluorinert. It appears to be important that the secondary fluid not wet the substrate in order to completely withdraw it from the main channel. This is shown in Figure 11, where the roles played by the Fluorinert and water shown in Figure 10 were reversed, i.e. the chip was prefilled with Fluorinert and water was loaded into the side channel. Parts 'a' through 'c' of Figure 11 show the water being pushed into the main channel. Parts 'd' through 'i' show the water being withdrawn from the main channel where the interface curvature is concave towards the Fluorinert as in Figure 10. Figure 11f shows the water about to break free of the main channel where there are still two interfaces within the main channel. These interfaces are about to make contact with each other at a point interior to the channel. As the water is drawn into the side channel these two interfaces make contact and when this happens most of the water breaks free of the main channel and pulls back into the side channel, but a small amount is left behind in the main channel attached to the wall opposite to the side channel, as shown in Figure 11g.

One final observation of the interface shapes shown in Figure 11 can be made. The direction of curvature of the interface in parts 'a-c' is opposite to that seen in parts 'd-g'. Variations in curvature can also be seen in the advancing and receding interfaces in Figure 10. Differences in advancing and receding contact angles have been reported in the literature [11] along with differences between dynamic and static contact angles [12]. According to these references, the source of the variation is the variable condition of the solid in contact with the interface. If the solid surface is hydrated due to recent contact with an aqueous fluid, for example, then the contact angle of an air/aqueous fluid interface with the solid decreases [13,14]. The system studied here is not a gas-liquid-solid system, rather it is a liquid-liquid-solid system, but similar phenomena are no doubt at play and may explain the variable curvature seen here. Thus, the contact angle is not constant, rather it depends on the movement of the interface and on the history of the solid surface in terms of fluids that have been in contact with it. Some attempts have been made to quantify the dependency of the contact angle on these conditions, but the results are for very specific systems and not for general purpose use. The contact angle affects the pressure differential across an interface, so while some successful examples of the use of capillary forces for microvalves have been reported, it appears that these forces cannot always be depended upon, particularly when a wetting fluid is injected and then withdrawn.

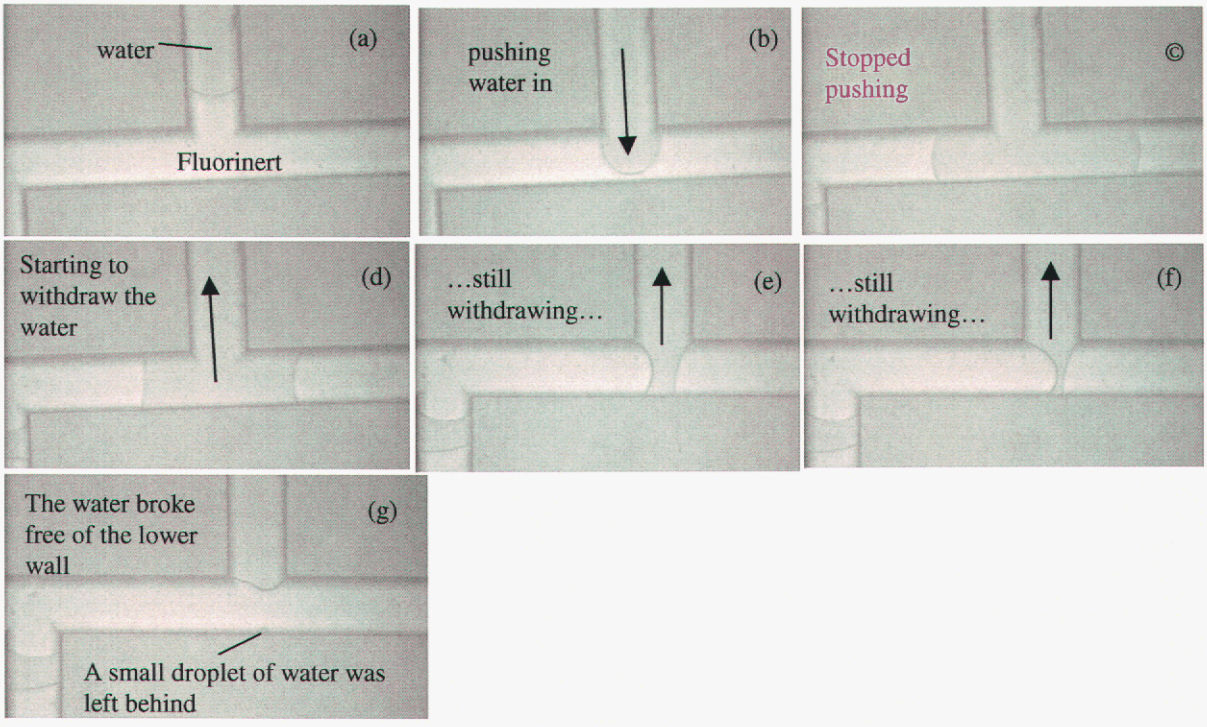

Figure 11. Photomicrographs showing the position of the water/Fluorinert interfaces as water is pushed out of a side channel and into a main channel, followed by withdrawing the water back into the side channel..

The method described above was used to control the positions of interfaces during testing of the valve where a plug of Fluorinert was used to break an electric circuit in a microchannel. Figure 12 shows a schematic of the experimental setup. The chip was prefilled with a phosphate buffer solution with a concentation 1 mM. Fluorinert is loaded into the first side channel. A voltage difference was applied between the end of the main channel and a second side channel. Figure 13 shows a photograph of the experimental setup.

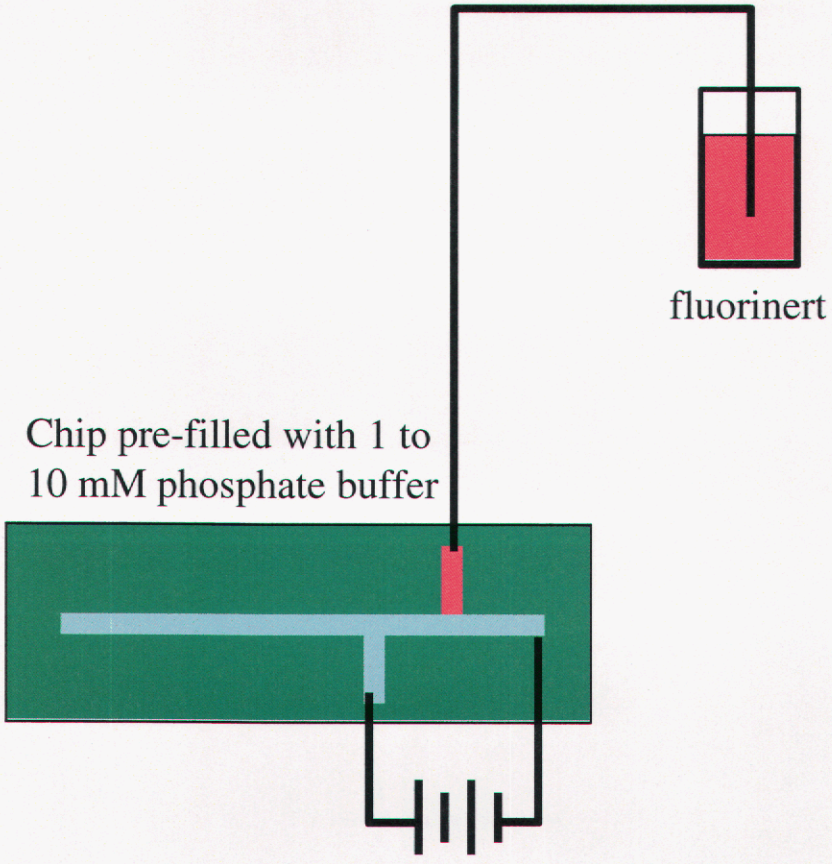

Figure 12. A schematic diagram of the experimental setup used to test the valve for stopping an electrical current.

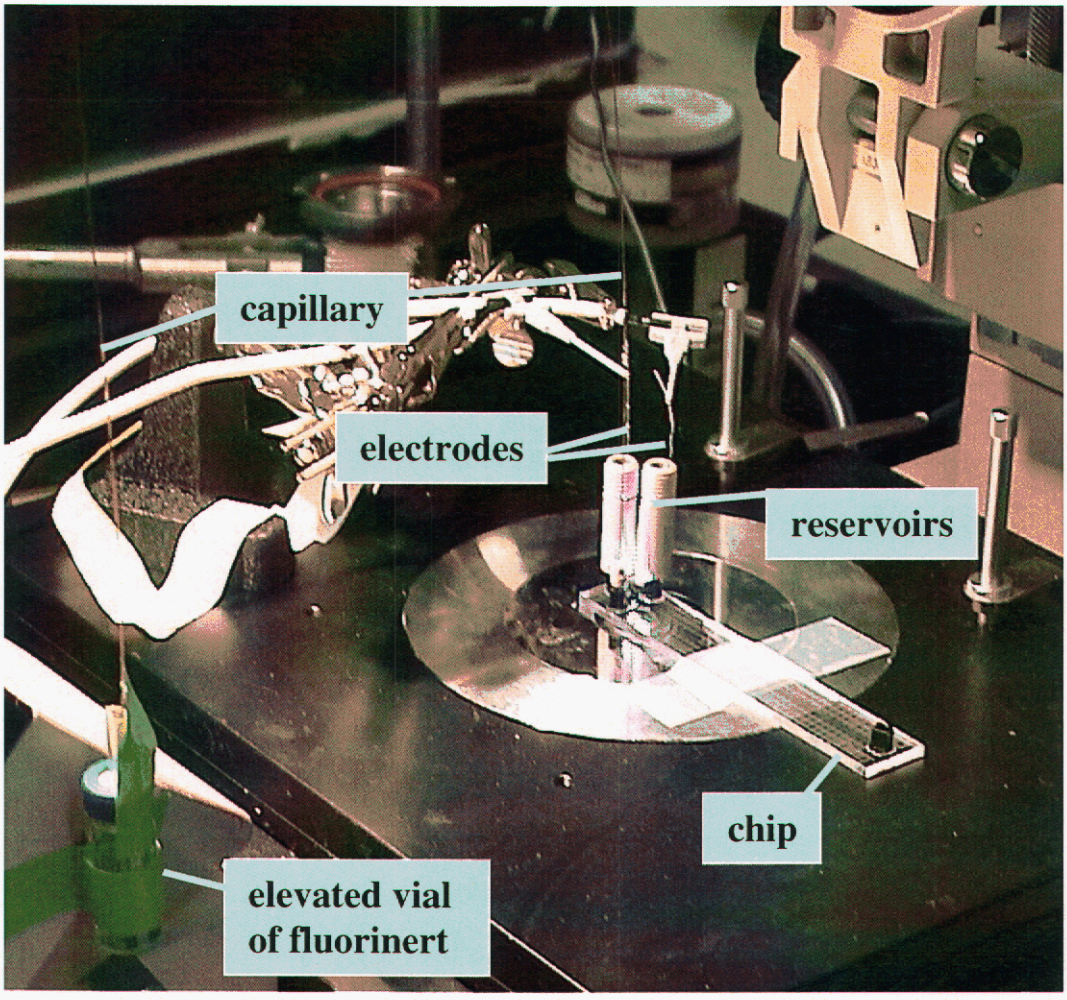

Figure 13. A photograph of the experimental setup used to test the valve for stopping an electrical current.

Results for the measured current as a function of the applied voltage are shown in Figure 14 for the valve in the open and closed states. As can be seen, closing the valve had very little effect on the current indicating that there was a current leakage path past the Fluorinert. This path appears to be provided by a narrow volume of buffer in the sharp corner regions of the microchannel, which spans the length of the Fluorinert plug as discussed below.

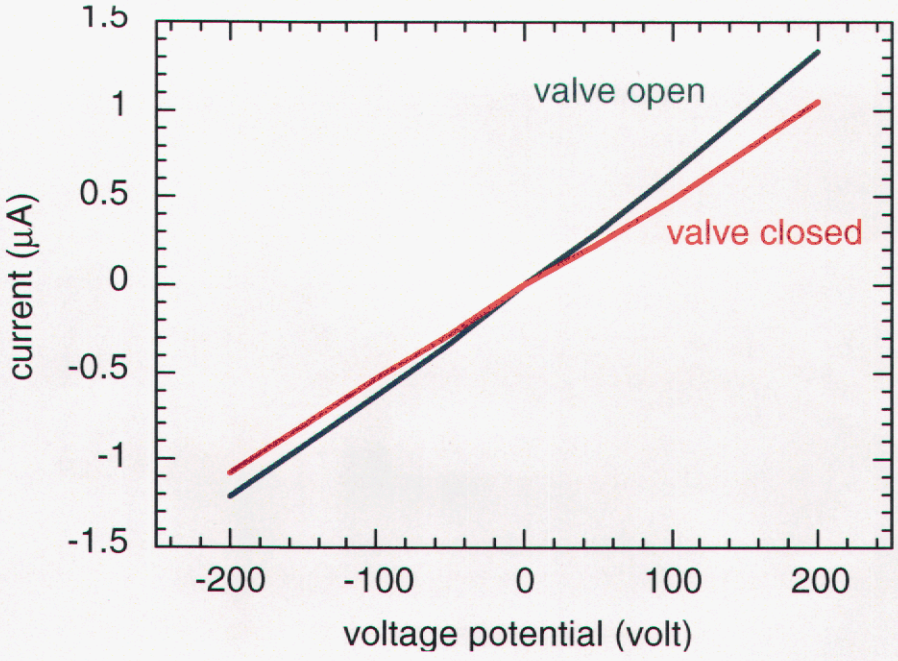

Figure 14. A plot of the measured current as a function of the applied voltage for the capillary valve in the opened and closed positions.

Figure 15 shows a schematic diagram of the leakage path past the Fluorinert that appears to exist. The microchannel is made in glass using an isotropic etching process. This results in a smooth channel cross section with rounded corners at the bottom of the channel as shown in the figure. Then a cover plate is bonded to the top of the chip, which creates sharp corners at the top of the channel cross section. The rounded corners are good because Fluorinert can stay in contact with them while it displaces the buffer even though the buffer wets the glass surfaces better. The sharp corners, however, create a wick that draws the buffer into them displacing Fluorinert as it goes. That is, since the buffer wets the glass channel better than Fluorinert the curvature of the interface results in a locally reduced pressure in the buffer. This curvature increases as the distance of the point of contact of the buffer with the wall, d (see Figure 15), gets smaller, as shown by Equation 4. This creates a pressure gradient acting to pull the buffer further into the corner region. Thus, the buffer wicks along the sharp corners past the Fluorinert providing a path for the current to bypass the buffer.

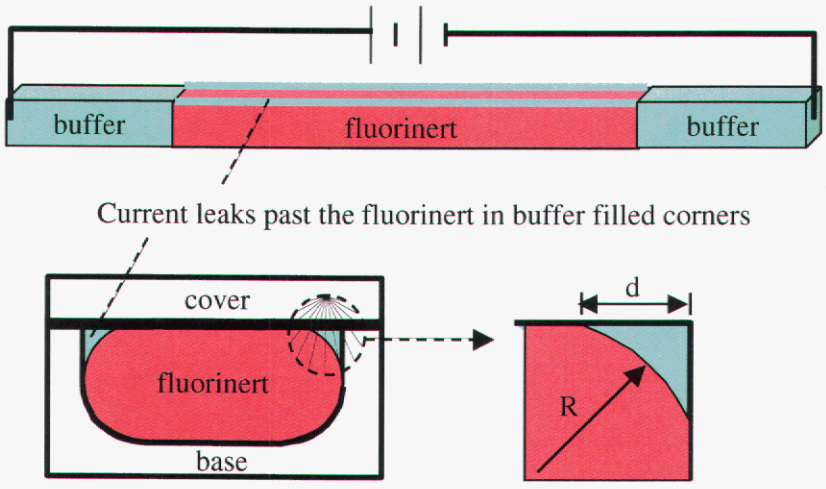

Figure 15. A schematic diagram of the buffer filled corner regions of the channel that provides a path for electrical current to flow past the Fluorinert.

$$R = \frac{d}{\cos\theta - \sin\theta} \qquad 4$$

Not only does current flow past the Fluorinert along these corner regions filled with buffer, the buffer itself can flow past the Fluorinert via these corner regions as well. This was confirmed in an experiment where fluorescent nanospheres were used to provide a flow tracer in the buffer. The buffer was observed to flow toward a plug of stationary Fluorinert on one end and it was observed to flow away from the Fluorinert on the other end. Figure 16 is a frame taken from a movie that showed the nanospheres emerging from the corner region of the buffer-Fluorinert interface.

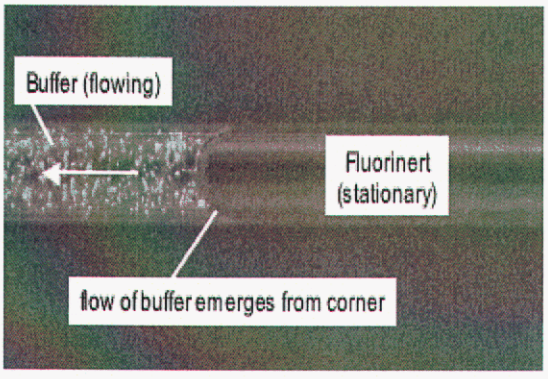

Figure 16. A photomicrograph of a Fluorinert plug in a microchannel and the buffer solution that flows past the Fluorinert via the channel corner regions.

To provide partial confirmation that the buffer in the regions of the sharp corners is the leakage path for electrical current past the Fluorinert, an experiment was carried out using microchannels constructed from capillaries and fittings. The capillaries have a circular cross section that is free of sharp corners. Figure 17 shows a photograph of a channel 'T' junction constructed for the experiment. The assembly was prefilled with buffer, and then Fluorinert was pushed into the side branch. The position of the leading Fluorinert interface was monitored using a microscope. The photograph on the lower right of the figure shows the leading interface of the Fluorinert in the side branch capillary while the Fluorinert is still stowed in the side branch. The photograph in the upper right shows the leading interface after the Fluorinert was pushed into the main branch where it was in position to stop the current flow.

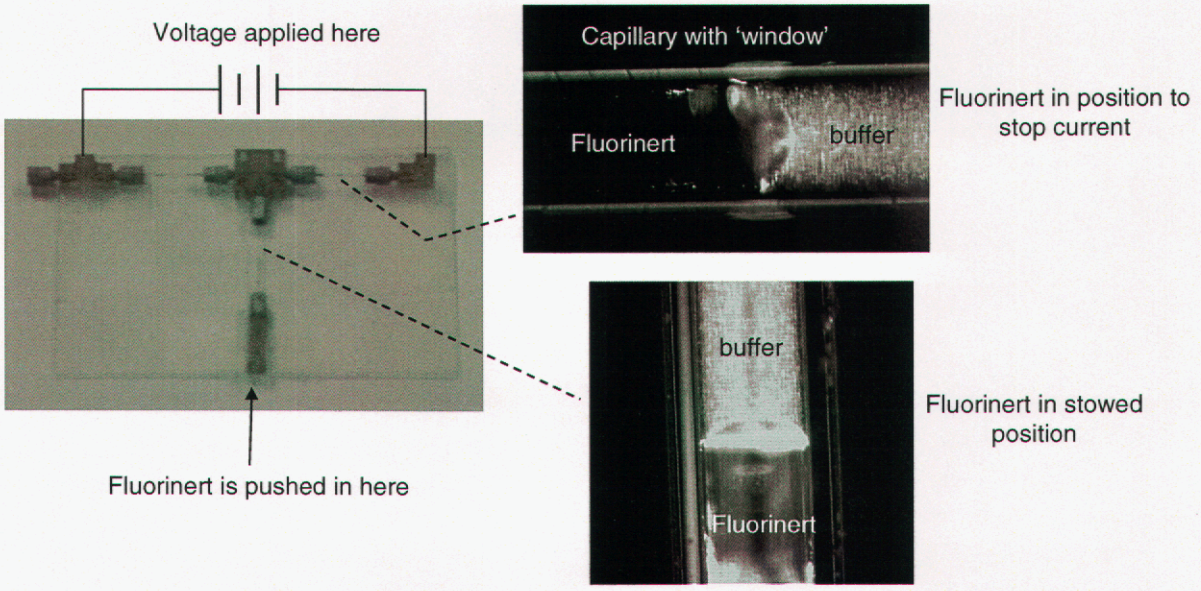

Figure 17. A photograph of the assembly of capillaries and fittings used to verify that in the absence of sharp corners in the capillaries the capillary valve will stop an electrical current.

A voltage difference was applied between the two ends of the main branch while the current along this branch was measured. Figure 18 shows that the current was roughly linear with voltage while the Fluorinert was stowed in the side branch (valve open) and it shows that the current was near zero when the Fluorinert was in the main branch (valve closed).

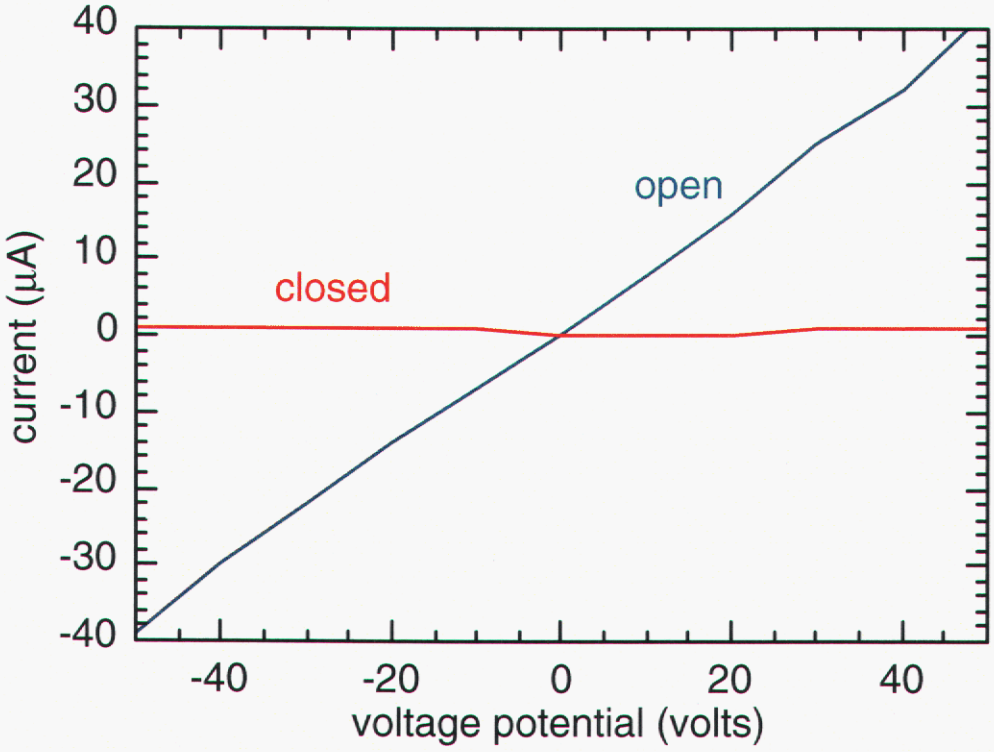

Figure 18. A plot of the measured current as a function of the applied voltage for the capillary valve in the opened and closed positions as implemented in an assembly of capillaries and fittings.

The above results show that the buffer filled corner regions that provide a leak path for current to flow past the Fluorinert can be prevented by eliminating the sharp corners in the channel cross section. This was done using capillaries with a circular cross section, but it could also be done with a double sided etch process where both the base and cover plates of a chip are etched as shown in Figure 19. While it appears that this would work, it results in a more expensive fabrication process. Consequently, another solution to the problem was identified as described below.

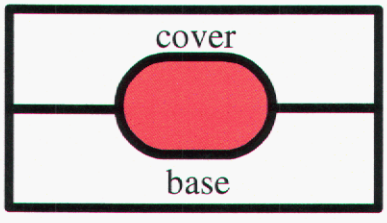

Figure 19. A schematic diagram showing how a two sided etch process can be used to eliminate sharp corners in a microchannel cross section.

One way of eliminating the buffer filled corner regions of the channel without eliminating the sharp corners is to apply a hydrophobic coating to the channel. This would increase the contact angle of the buffer with the glass allowing the Fluorinert to better wet the glass. The coating can be applied by exposing the channel surfaces to a tridecafluorooctyl silica solution, as desribed in [15]. The coating was applied to all channel surfaces, although it would only be necessary (and perhaps preferrably) to coat the channel in the vicinity of the valve itself. A chip with a simple side channel intersecting a main channel was not available, so one with two channels crossing was used. This increased the complexity of controlling the position of the Fluorinert, but it was still workable. Using the experimental setup shown in Figure 12, and a chip with the hydrophobic coating, the valve was tested for its capability to break the circuit. Figure 20 shows the Fluorinert stowed in one of the channel arms that served as the side channel, and it shows the Fluorinert after it was pushed out into the main channel. Note the interface in the main channel is now concave towards the buffer, a signature of the presence of the hydrophobic coating. That is, the Fluorinert is now the wetting fluid. Of course, this will result in leaving a small amount of residual Fluorinert in the main channel upon withdrawal to the side channel, as discussed for Figure 11. It remains to be seen how much of a problem this causes.

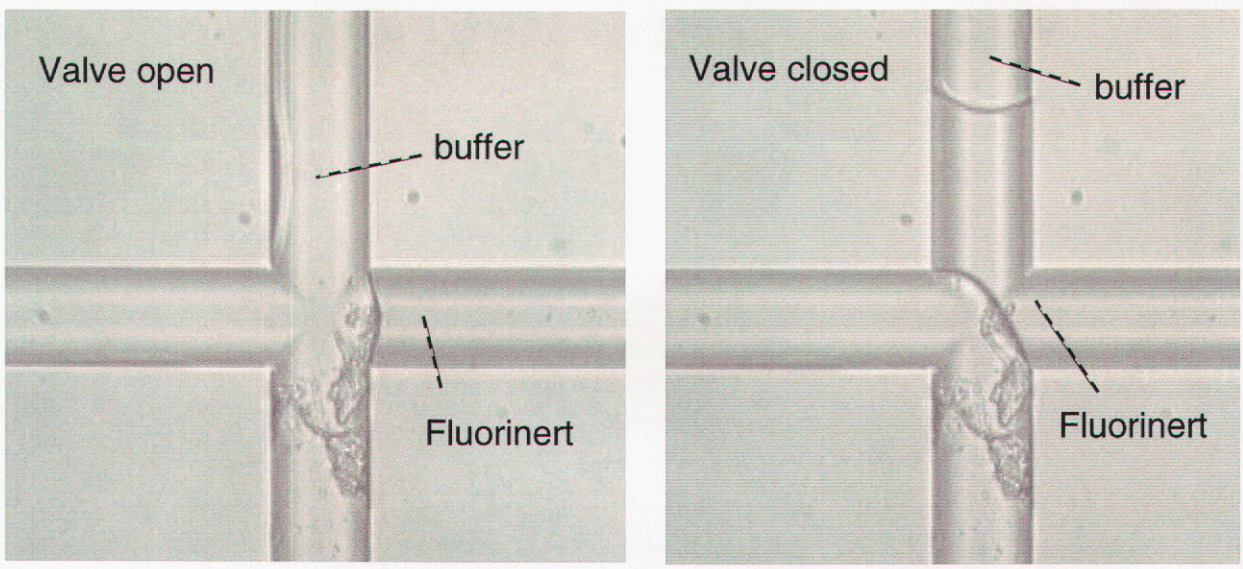

Figure 20. Photomicrographs showing Fluorinert before and after it was pushed out of a side channel and into a main channel where the channel surfaces were given a hydrophobic coating.

Figure 21 shows the current measured along the main channel, where the valve started out open, then it was closed, and then it was opened and closed three more times. The valve in the closed position reduces the current by over two orders of magnitude.

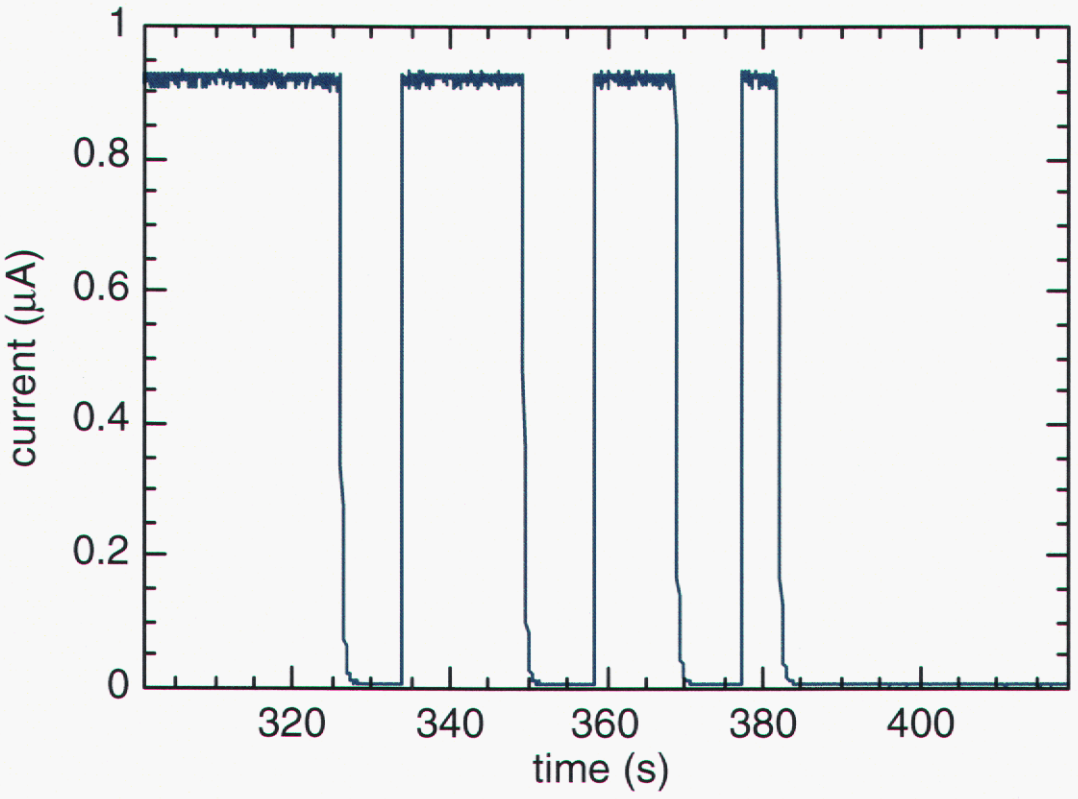

Figure 21. A plot of the measured current flowing through the main channel for an applied voltage of 100 V for several cycles of pushing the Fluorinert into the main channel and then withdrawing it.

During the course of these experiments some interesting behavior of the Fluorinert/buffer interface was noted as shown in Figure 22. When the voltage was turned off the curvature of the interfaces appeared approximately uniform, but when the electric field in the Fluorinert plug was sufficiently high (~1000 V/mm) the curvature was more concentrated near the center of the interface with near straight sections extending to the channel walls. This appears to be an electrowetting or related nonlinear effect. When the field was raised ~20% higher, the Fluorinert plug moved toward the top of the image in Figure 22.

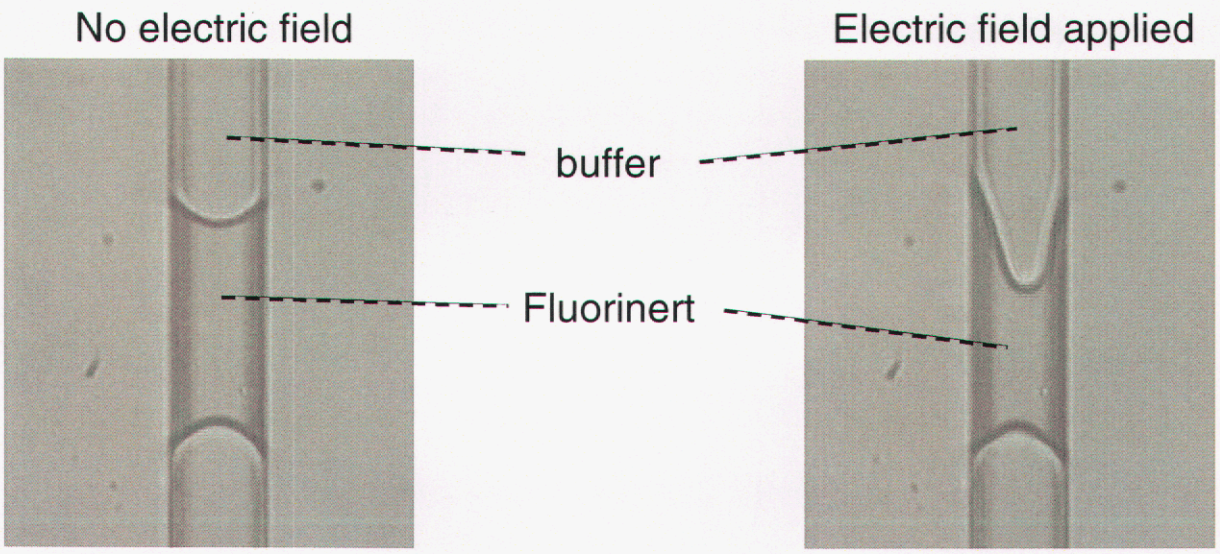

Figure 22. The shapes of Fluorinert/buffer interfaces is affected by the application of a strong electric field. At a slightly higher applied field, the Fluorinert plug moves toward the top of the image.

6. Conclusions

The experiments described demonstrate that the position of a dielectric fluid can be controlled in a microchannel and used to break an electric circuit. They also demonstrate that this secondary fluid remains intact so that it can be moved reversibly between a stowed position and a position where it can stop a flow. The wetting behavior of the secondary fluid was found to play an important role. Here, the secondary fluid is said to wet the channel walls when the interface between the primary and secondary fluids made a contact angle less than 90^{o} as measured on the secondary fluid side. If the secondary fluid did not wet the channel walls the primary fluid wicked along sharp corners in the channel past the secondary fluid resulting in a short circuit for electric current to flow past it. By making a hydrophobic coating on the interior surfaces of the channel the secondary fluid, Fluorinert, did not wet the walls. No electrical short circuit was detected under these conditions. However, when the secondary fluid wets the walls it cannot be completely withdrawn from the main channel, where a small chunk is left behind.

A simplified model was used to develop designs for the capillary valve that could be actuated with an electrokinetic pump, i.e. they could be actuated with an electrical signal. But, the experiments showed that the contact angle may not always be constant, which could defeat designs that rely on capillary forces to hold and move the secondary fluid. If the capillary forces do not work then other methods could be used to control the position of the secondary fluid. These include electrowetting, electrocapillary and dielectrophoretic methods. Finally, another method that could be used is a reversible electrokinetic pump to shuttle the secondary fluid into and out of the stowed position.

The next steps for developing the valve concept studied here include the following. Detailed investigations for controlling the movement and position of the secondary fluid should be carried out. This would include experiments measuring the speed of actuation of the valve. Custom designed microchannels should be fabricated with 'necks' to set limits on the range of motion of the secondary fluid. Applications of the valve to gas phase systems should be investigated in more detail, including the measurements of the pressure differentials that a liquid (secondary fluid) could support in a channel.

Several other applications of immiscible liquids in microchannels were identified in this work. One is a method for mixing and transporting reagents in microchannels with low dispersion. The reagent mixture is 'sandwiched' between two plugs of Fluorinert and the assembly is pushed along the channel with a pressure gradient. The combination of the motion and the near shear free interfaces bounding the ends of the reagent mixture results in a recirculating flow field within it that produces accelerated mixing therein, as described in the appendix to this report.

A second application is for a dielectrophoretic process, where Fluorinert is partially extruded from a side channel into a main channel thereby forming a constriction. When combined with an electric field the constriction creates gradients in the field that can be used to dielectrophoretically trap particles depending on their size and other characteristics. Such an application could be used to sort particles so that subsets of them could be subjected to further analyses. This would be a unique implementation of dielectrophoresis where the size of the constriction, and hence the degree of particle trapping, could be adjusted during the process.

References

[1] T. Strobelt, M. Willmann, J. Kohnle, G. Waibel, H. Sandmaier, and R. Zengerle, "Energy optimized valve with low leakage rates", Micro-Electro-Mechanical Systems, ASME, 2000.

[2] P.F. Man, C.H. Mastrangelo, M.A. Burns, and D.T. Burke, "Microfabricated capillary-driven stop valve and sample injector", IEEE, 1998.

[3] S.H. Lee, C.S. Lee, B.G. Kim, and Y.K. Kim, "Quantitatively controlled nanoliter liquid manipulation using hydrophobic valving and control surface wettability", *J. Micromech. Microeng.*, **13**:89-97, 2003.

[4] H. Andersson, W. van der Wijngaart, P. Griss, F. Niklaus, and G. Stemme, "Hydrophobic valves of plasma deposited octafluorocyclobutane in DRIE channels", *Sensors and Actuators*, **75**:136-141, 2001.

[5] Q. Yu, J.M. Bauer, J.S. Moore, and D.J. Beebe, "Fabrication and characterization of a biomimetic hydrogel check valve", in *Microtechnologies in Medicine & Biology*, pp. 336-339, IEEE, 2000.

[6] E.F. Hasselbrink, T.J. Shepodd, and J.E. Rehm, *Analytical Chemistry*, **74**:4913-4918, 2002.

[7] Fluorinert electronic liquid, 3M, 3M Center, Building 223-6S-04, St. Paul, MN 55144-1000.

[8] M.W. Prins, W.J.J. Welters, and J.W. Weekamp, "Fluid control in multichannel structures by electrocapillary pressure", *Science*, **291**:277-280, 2001.

[9] C.J. Kim, "Microfluidics using the surface tension force in microscale", in *Microfluidic Devices and Systems*, C.H. Mastrangelo and H. Becker Eds., pp. 49-55, SPIE, 2000.

[10] K. Handique, D.T. Burke, C.H. Mastrangelo, and M.A. Burns, "Nanoliter liquid metering in microchannels using hydrophobic patterns", *Analytical Chemistry*, **72**:4100-4109, 2000.

[11] C.W. Extrand, "Water contact angles and hysteresis of polyamide surfaces", *J. Colloid and Interface Sci.*, **248**:136-142, 2002.

[12] V.D. Sobolev, N.V. Churaev, M.G. Velarde, and Z.M. Zorin, "Surface tension and dynamic contact angle of water in thin quartz capillaries", *J. Colloid and Interface Sci.*, **222**:51-54, 2000.

[13] B. Janczuk, W. Wojcik, and A. Zdziennicka, "Wettability and surface free energy of glass in the presence of cetyltrimethylammonium bromide", *Materials Chemistry and Physics*, **58**:166-171, 1999.

[14] T. Englander, D. Wiegel, L. Naji, and K. Arnold, "Dehydration of glass surfaces by contact angle measurements", *J. Colloid and Interface Sci.*, **179**:635-636, 1996.

[15] B.J. Kirby, D.S. Reichmuth, R.F. Renzi, T.J. Shepodd, and B.W. Wiederman, "Microfluidic routing of aqueous and organic flows at high pressures: Fabrication and characterization of integrated polymer microvalve elements", submitted to *Lab on a Chip*, July, 2004.

[16] T.B. Jones, "Liquid dielectrophoresis on the microscale", *J. Electrostatics*, **51-52**:290-299, 2001.

[17] M.R. Bringer, C.J. Gerdts, H. Song, J.D. Tice, and R.F. Ismagilov, "Microfluidic systems for chemical kinetics that rely on chaotic mixing in droplets", *Phil. Trans. R. Soc. Lond.* A **362**, 1087-1104, 2004.

[18] R.B. Bird, W.E. Stewart, and E.N. Lightfoot, *Transport Phenomena, Second Edition,* John Wiley and Sons Inc., 2002.

[19] J.M. Ottino, *The kinematics of mixing: stretching, chaos, and transport,* Cambridge University Press, 1989.

[20] J.M. Ottino and S. Wiggins, "Introduction: mixing in microfluidics", *Phil. Trans. R. Soc. Lond.* A **362**, 923-935, 2004.

[21] P.R. Schunk, P.A. Sackinger, R.R. Rao, K.S. Chen, T.A. Baer, D.A. Labreche, A.C. Sun, M.M. Hopkins, S.R. Subia, H.K. Moffat, R.B. Secor, R.A. Roach, E.D. Wilkes, D.R. Noble, P.L. Hopkins, and P.K. Notz, 2002 "GOMA 4.0 -- A Full-Newton Finite Element Program for Free and Moving Boundary Problems with Coupled Fluid/Solid Momentum, Energy, Mass, and Chemical Species Transport: User's Guide, Volume 1: Problem Description". Technical Report SAND 2002-3204/1, Sandia National Laboratories, Livermore, CA, October 2002.

[22] P.R. Schunk, P.A. Sackinger, R.R. Rao, K.S. Chen, T.A. Baer, D.A. Labreche, A.C. Sun, M.M. Hopkins, S.R. Subia, H.K. Moffat, R.B. Secor, R.A. Roach, E.D. Wilkes, D.R. Noble, P.L. Hopkins, and P.K. Notz, 2002 "GOMA 4.0 -- A Full-Newton Finite Element Program for Free and Moving Boundary Problems with Coupled Fluid/Solid Momentum, Energy, Mass, and Chemical Species Transport: User's Guide, Volume 2: Material Description". Technical Report SAND 2002-3204/2, Sandia National Laboratories, Livermore, CA, October 2002.

[23] H.A. Stone, A.D. Stroock, and A. Ajdari, Engineering flows in small devices. *A. Rev. Fluid. Mech.* 36, 381-411, 2004.

Appendix: A bolus flow for low dispersion transport and mixing of reagents

One of the important accomplishments of this project was the development of a method to control the positions and movements of individual liquids in a system of immiscible liquids. This method can be used to develop other microfluidic processes that would advance Sandia's capability in the general area of microfluidics. One of these is a mixing process. A detailed analysis of the mixing provided by a bolus flow is described below.

Mixing in microfluidics

During the course of conducting chemical and biological analyses in a microfluidic system it is usually necessary at some point to add reagents to a small volume sample and mix them. Despite the inherently small length scales involved in microfluidic applications, efficient mixing remains a challenging problem [17]. Typical numbers for a characteristic length, kinematic viscosity, and velocity, are respectively, $H = 10^{-3}$ to 10^{-2} cm, $\nu = \mu/\rho = 10^{-2}$ cm^2/s, $U = 10^{-1}$ to 1 cm/s, and yield a Reynolds number $UH/\nu = 10^{-2}$ to 1. Therefore, flows in microfluidic channels are typically dominated by viscous forces and the possibility of enhanced mixing through the generation of turbulence does not exist in normal applications. Additionally, typical coefficients of molecular diffusion, D, vary between 10^{-7} cm^2/s (large molecules) and 10^{-5} cm^2/s (small molecules), so that ratios of advection to diffusion time scales for flows in microfluidic channels, as characterized by the Péclet number, UH/D, vary from 10 to 10^5 [18]. For two miscible and laminar fluid streams flowing side by side in a microchannel, the time for each species to penetrate a half channel width is roughly $t = H^2/D$, which, for streams moving at a constant velocity, U, would require a channel length of 10^{-2} to 10^3 cm. Thus, in spite of the small length scales, diffusion alone may not be sufficient to mix two fluids in a reasonable distance within a microfluidic device.

A bolus flow

Consider a small plug of liquid in a microchannel with an immiscible fluid bounding it on both sides. As the small plug, or bolus, of fluid travels down the microchannel an internal circulatory flow develops due to the no-slip and no penetration conditions experienced at the bolus interfaces. This circulatory flow was confirmed in a visualization experiment using a bolus of water and fluorescent nanospheres in a pressure-driven fluorinert host fluid. Figure 23 shows both an image of the actual fluorinert, water bolus, fluorinert configuration and a schematic of the observed particle path lines within the water bolus for the configuration in motion from right to left. Due to the internal circulatory flows within a bolus moving at a constant velocity, which enhances the diffusion with advection across the bolus cross-section, the time and distance required to fully mix two initially unmixed fluid species may be much shorter. Moreover, the finite axial length of the bolus, L, typically no more than an order of magnitude larger than the characteristic width of the microchannel, requires much smaller volumes of fluid sample or reagent, a particularly attractive feature for microfluidic applications [19]. An analysis of the mixing of two miscible but initially distinct fluid species was performed for a bolus moving at constant velocity within a straight microchannel of constant cross-section.

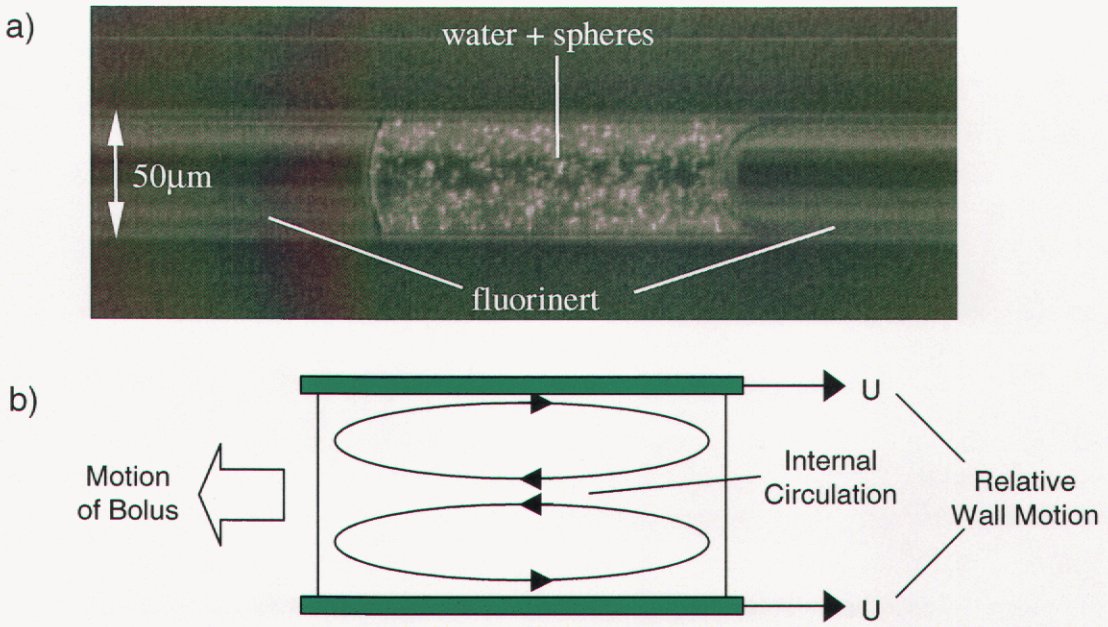

Figure 23. a) A bolus moving from right to left in a microchannel. b) Internal circulation within bolus due to no-slip conditions at walls.

System model

In this preliminary analysis characterizing the mixing in bolus flows the model was restricted to two dimensions. Such a simplified model is applicable to boluses moving within rectangular microchannels whose cross-sectional width, W, is much larger than its height, H, as shown in Figure 24. Under these conditions significant transport only occurs in the y-z plane.

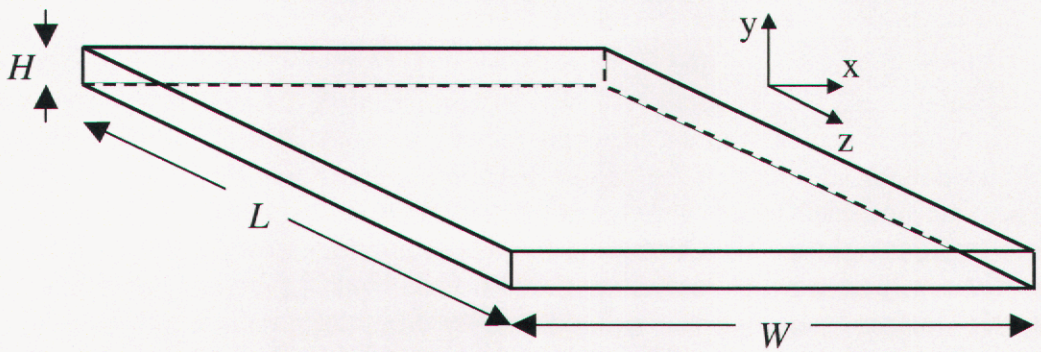

Figure 24. Rectangular microchannel geometry with $H << W$ for pressure-driven flow in the z-direction. The bolus has a length L.

Further simplification is made by assuming symmetry across the mid-plane of the channel (at height $H/2$) and assuming that the ends of the bolus are flat with no curvature along either of the principal axes perpendicular to the z-axis. Figure 25 shows a schematic of the model bolus geometry in its initial configuration, with two miscible fluid species positioned one in front of the other along the z-axis. Any inertial effects are taken to be negligible due to the small Reynolds number, and a reference frame was chosen to move at a constant velocity, U, equal to the assumed velocity of the bolus. In this reference frame the boundary conditions are more easily applied to the exterior surfaces of the bolus.

The equations of change governing the transport of momentum and mass within the bolus are the incompressible Navier-Stokes equations and the species transport equation. These equations may be nondimensionalized with a length scale, H, and velocity scale, U, to yield the following forms [20]:

$$\nabla \cdot \mathbf{v} = 0, \tag{5}$$

$$\mathrm{Re}\left(\frac{\partial \mathbf{v}}{\partial t} + \mathbf{v} \cdot \nabla \mathbf{v}\right) = -\nabla p + \nabla^2 \mathbf{v}, \tag{6}$$

$$\frac{\partial c}{\partial t} + \mathbf{v} \cdot \nabla c = \frac{1}{\mathrm{Pe}} \nabla^2 c, \tag{7}$$

where $\mathrm{Re} = UH/\nu$ and $\mathrm{Pe} = UH/D$ are respectively the Reynolds and Péclet numbers. An additional nondimensional parameter, ε^{-1} = L/H, the aspect ratio, which appears in the boundary conditions, was set to one for all calculations. The bolus was assumed to be initially at rest ($\mathbf{v} = \mathbf{0}$) with an initial species concentration value of 1.0 for $0.0 \le z \le 0.5$ and 0.0 for $0.5 < z \le 1.0$.

To simulate the right-to-left, pressure-driven motion of the bolus no-slip boundary conditions were applied to the velocity field, $\mathbf{v}(y, z, t)$ and a no flux boundary condition was applied to the concentration field $c(y, z, t)$:

$$\mathbf{v} = 1, \quad \text{for} \quad 0 \le z \le 1 \quad \text{at} \quad y = 1, \tag{8}$$

$$\frac{\partial \mathbf{v}}{\partial y} = 0, \quad \text{for} \quad 0 \le z \le 1 \quad \text{at} \quad y = 0, \tag{9}$$

$$\frac{\partial \mathbf{v}}{\partial z} = 0, \quad \text{at} \quad z = 0 \text{ and } 1 \quad \text{for} \quad 0 \le y \le 1, \tag{10}$$

$$\mathbf{n} \cdot \nabla c = 0 \quad \text{on all boundaries.} \tag{11}$$

The above governing equations and boundary conditions were solved numerically using the Sandia in house code, Goma [21,22].

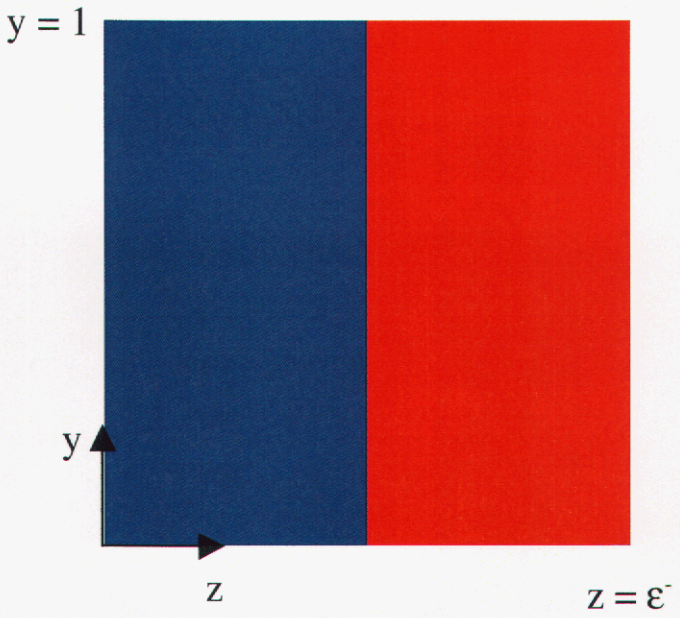

Figure 25. Initial nondimensional concentration field (blue = 1.0 and red = 0.0).

A typical contour plot of the streamfunction is shown in Figure 26 and reveals a steady circulatory flow field within the bolus. This flow field establishes itself almost instantaneously and serves to "mix" the initially "unmixed" species. Figure 26 shows an example concentration snapshot for a large Péclet number after the bolus has traveled down the channel many bolus lengths.

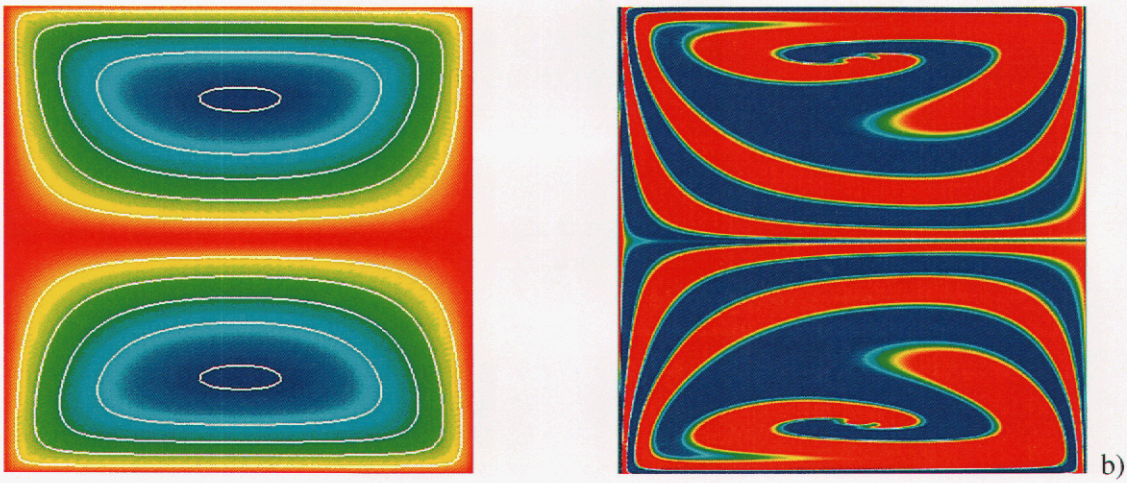

Figure 26. a) Contours of streamlines for bolus flow with $\mathrm{Re} = 1.0$. b) Concentration field snapshot at nondimensional time $t^* = tU/H = 24$ for $\mathrm{Pe} = 10^7$ (blue = 1.0 and red = 0.0).

One quantitative measure of the mixing, appropriate for the miscible system of interest here [23], is the mixing index, $M(t)$, defined by

$$M(t) = 1 - \frac{\sigma(t)}{\sigma_o}, \tag{12}$$

where $\sigma(t)$ is the square root of the average variance of concentration from its equilibrium value. For two-dimensional systems the square root of the average variance of concentration is defined by the expression

$$\sigma(t) = \int_A \left| c(y,z,t) - c_\infty \right| dA \tag{13}$$

with σ_o is its initial value when $c(y,z,t=0) = c_o(y,z)$. At concentration equilibrium, when the concentration field is fully mixed, $c(y,z,t \to \infty) = c_\infty$. For the initial species concentration in Figure 25, the equilibrium concentration c_∞ will eventually have a value of 0.5. The initial average variance of concentration σ_o therefore has a value of 0.5 for the nondimensional bolus geometry with unit area. The transient mixing index value varies from an initial value of 0.0 (unmixed) to an asymptotic value of 1.0 (fully mixed). This definition of the mixing index was used to characterize the mixing in bolus flows for a wide range of Péclet numbers, as detailed below.

Results

Figure 27 shows the value of the mixing index versus nondimensional time for Péclet numbers between 10 and 10^4. In all calculations the Reynolds number and aspect ratio, ε^{-1}, were assumed to have a value of one. For boluses with an aspect ratio of one, the data in Figure 27 may alternatively be interpreted as the value of the mixing index as a function of the number of nondimensional bolus lengths traveled down the microchannel. For $\mathrm{Pe} = 10$ the bolus was fully mixed after traveling approximately five nondimensional bolus lengths, or a dimensional distance $5H$. For $\mathrm{Pe} = 10^4$ the bolus needed to travel nearly 50 nondimensional bolus lengths, or a dimensional distance $50H$, to become fully mixed. For an example channel height of $H = 10^{-2}$ cm, these distances have numerical values of roughly 10^{-2} cm and 1 cm, respectively. These lengths should be compared to the previous estimates of 10^{-2} cm (for Pe = 10) and 10 cm (for Pe = 10^4) for typical side-by-side fluid stream mixing where there is little or no convective transport between species.

These preliminary calculations suggest that, for the majority of Péclet numbers of interest in microfluidic applications, mixing two fluid species within a finite bolus can decrease the length of microchannel and time required for mixing by up to an order of magnitude. Further analysis is needed to more fully characterize the effects of different aspect ratios, bolus end curvatures, and a three dimensional geometry on the mixing in pressure-driven boluses in microchannels.

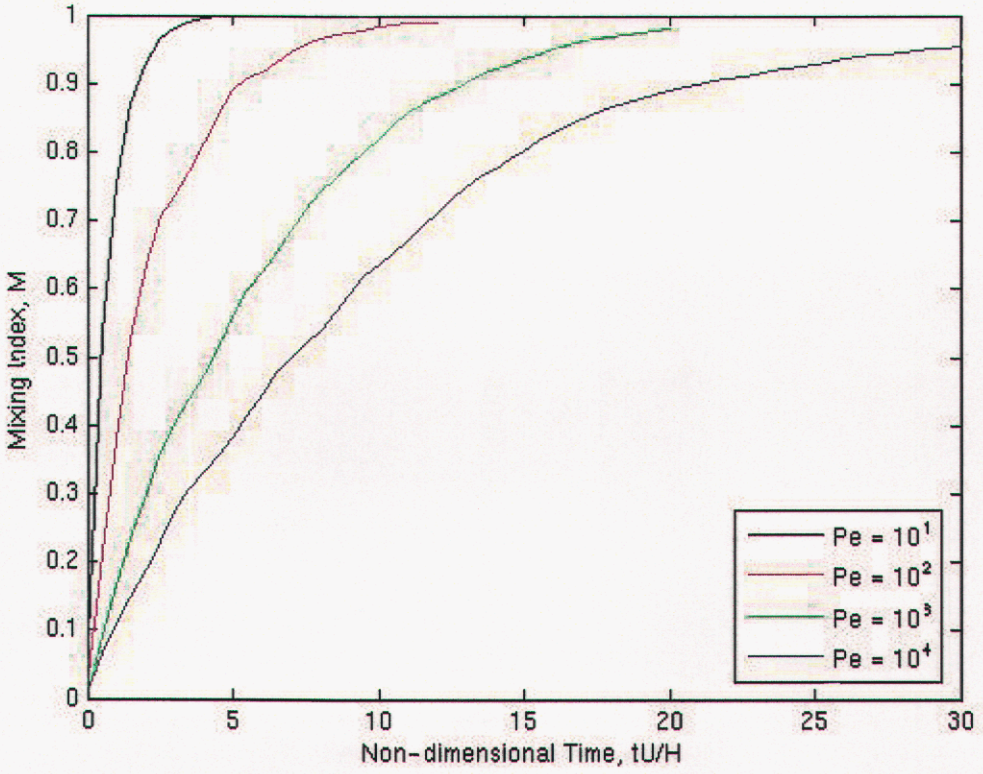

Figure 27. A plot of mixing index, $M(t)$, versus time for various values of Péclet number.

Acknowledgement

The authors would like to gratefully acknowledge the assistance of Russell A. Whitesides and Patricia L. Rahm for the calculations they carried out in support of the analysis of mixing in Bolus flows.

Distribution

1	MS 0825	W. L. Hermina	
1	MS 0834	R. C. Givler	
1	MS 0834	J. S. Lash	
1	MS 9404	G. D. Kubiak, 08750	
		Attn: MS 9401	J. E. M Goldsmith, 08751
		MS 9401	G. F. Cardinale, 08753
		MS 9409	P. A. Spence, 08754
1	MS 9042	S. K. Grifftihs	
10	MS 9042	M. P. Kanouff	
1	MS 9042	C. D. Moen	
1	MS 9042	R. H. Nilson	
5	MS 9042	B. M. Rush	
1	MS 9403	J. M. Hruby	
3	MS 9951	E. B. Cummings	
1	MS 9951	Y. Fintschenko	
1	MS 9951	A. E. Pontau	
1	MS 9953	R. W. Crocker	
1	MS 9953	J. A. Lamph	
1	MS 0188	D. Chavez, LDRD Office, 1011	
1	MS 0899	Technical Library, 9616	
3	MS 9018	Central Technical Files, 8945-1	
1	MS 9021	Classification Office, 8511 for Technical Library, MS 0899, 9616	
	MS 9021	Classification Office, 8511 for DOE/OSTI via URL	

Intentionally Left Blank